

Core Bifiltration

Nello Blaser¹, Morten Brun², Odin Hoff Gardaa¹, and Lars M. Salbu²

¹Department of Informatics, University of Bergen, Norway

²Department of Mathematics, University of Bergen, Norway
 {nello.blaser,morten.brun,odin.garda,lars.salbu}@uib.no

Abstract

The motivation of this paper is to recognize a geometric shape from a noisy sample in the form of a point cloud. Inspired by the HDBSCAN clustering algorithm and the multicover bifiltration, we introduce the core- and the alpha-core bifiltrations. The multicover-, core- and alpha-core bifiltrations are all interleaved, and they enjoy similar Prohorov stability properties. We have performed experiments with the core and the alpha-core bifiltrations where we have calculated their persistent homology along lines in the two-dimensional persistence parameter space.

2020 Mathematics Subject Classification: 55N31, 62R40.

Keywords: Multicover Bifiltration, Multiparameter Persistence, Stability

1 Introduction

Multiparameter persistent homology has recently emerged as an important part of topological data analysis [3]. In multiparameter persistent homology, we study the changes in homology of a topological space equipped with a multiparameter filtration as these parameters vary. In practice, many filtrations have two parameters, so-called bifiltrations. Examples include the degree-Rips bifiltration [11, 2], the density-Rips bifiltration [3, 6] and the multicover bifiltration [15]. The study of different bifiltrations and their relationships with each other is an active research area. In this paper, we introduce the core bifiltration of a finite set of points in a metric space.

We introduce the core bifiltration together with a variant built on the alpha-complex, the alpha-core bifiltration, both of which are interleaved with the multicover bifiltration. This interleaving allows us to transfer stability results from [2], in a weakened form, from the multicover bifiltration to the alpha-core bifiltration. We also establish stability results for the core bifiltration similarly. Like the degree-Rips bifiltration, the core bifiltration is computationally more accessible than the multicover bifiltration. There are ongoing efforts in the research community aiming to improve the feasibility of computing the multicover bifiltration through techniques such as, for example, sparsification [4] and exploring related combinatorial bifiltrations [7, 8, 9].

Contributions. Our contributions are as follows.

1. We introduce two bifiltrations of spaces, namely the *core bifiltration* and the *alpha-core bifiltration*. These are inspired by the density-dependent clustering algorithm HDBSCAN [5].
2. In the Theorems 3.7 and 4.5 we describe interleavings between the (alpha-) core and multicover bifiltrations summarized in the following diagram of inclusions:

$$\begin{array}{ccc}
 & \text{Cov}_{2r,k}(A) & \\
 & \subsetneq & \supsetneq \\
 \alpha\text{Cr}_{r,k}(A) \subseteq \text{Cr}_{r,k}(A) & & \alpha\text{Cr}_{4r,k}(A) \subseteq \text{Cr}_{4r,k}(A), \\
 & \supsetneq & \subsetneq \\
 & \alpha\text{Cr}_{3r,k}(A) &
 \end{array}$$

where $\text{Cr}_{r,k}(A), \alpha\text{Cr}_{r,k}(A), \text{Cov}_{r,k}(A) \subseteq \mathbb{R}^n$ denote the core, alpha-core and multicover bifiltrations, of a finite subset $A \subseteq \mathbb{R}^n$ in filtration degree $(r, k) \in \mathbb{R}^2$, respectively. Here the parameter r corresponds to the radius parameter in the Čech complex, and k is a density parameter. See Figure 1 for a toy example where the core- and multicover bifiltrations differ.

3. For each filtration value (r, k) , the core bifiltration admits a cover consisting of metric balls. This allows us to apply the standard nerve lemma to get that the core bifiltration is homotopy equivalent to the geometric realization of the core Čech bifiltration denoted $\text{cC}_{r,s}(A)$. A similar argument is also done for the alpha-core bifiltration.
4. Using an approach similar to Blumberg and Lesnick [2] we get a Prohorov stability result for the core and alpha-core bifiltrations.
5. We have performed experiments¹ on synthetic point clouds. For each point cloud, we compute the alpha-core persistent homology both for a horizontal line with a fixed k parameter and along a line with a negative slope. In both cases, we compute the bottleneck distance between the persistence diagram of a noisy sample to the persistence diagram of a sample without noise.

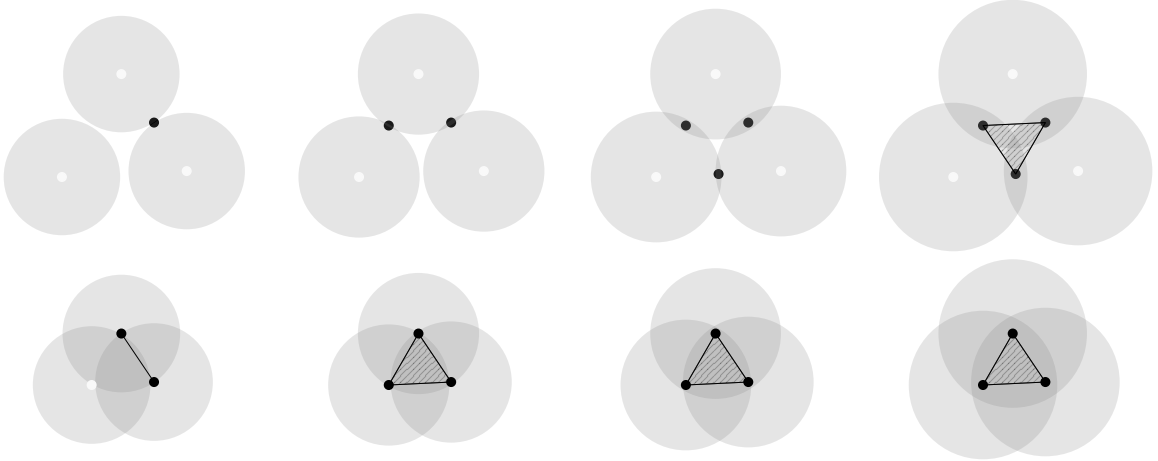


Figure 1: Let $A = \{(0, 0), (1, \sqrt{3}), (2.1, 0.1)\} \subseteq \mathbb{R}^2$. For a fixed k , the multicover filtration $\text{Cov}_{r,k}(A)$ admits a covering consisting of k -intersections of balls. The top row shows the filtered nerve of this covering of $\text{Cov}_{r,2}(A)$, whereas the bottom row shows the core Čech filtration $\text{cC}_{2r,2}(A)$ with the radius parameter r increasing from left to right.

This manuscript is structured as follows: In Section 2, we review some notions relevant to multi-parameter persistent homology, including a formal definition of the multicover bifiltration. Section 3 defines the core dissimilarity and its corresponding core bifiltration and shows the interleaving to the multicover bifiltration. In Section 4, we introduce the alpha-core bifiltration and show how it is related to the core bifiltration and the multicover bifiltration. Stability results are shown in Section 5. In Section 6, we showcase properties of the alpha-core bifiltration in some experiments on noisy point cloud datasets. Finally, we conclude the paper in Section 7.

2 Background

Let P be a partially ordered set, or **poset**. A **filtration** (of sets) over P is a collection of sets $C = \{C_p\}_{p \in P}$ where $C_p \subseteq C_{p'}$ whenever $p \leq p'$. For a poset P , we let P^{op} denote the **opposite poset** with the same underlying set P but with the order reversed, i.e., $p \leq q$ in P^{op} if $q \leq p$ in P . For posets P and Q , we can form the **product poset** $P \times Q$, where $(p, q) \leq (p', q')$ if both $p \leq p'$ and $q \leq q'$.

A **simplicial complex** is a pair (K, V) where V is a set (called the **vertex set**) and K is a set of finite subsets of V (called **simplices**) such that if σ is a simplex in K and $\tau \subseteq \sigma$ then τ is

¹The implementation is available at <https://github.com/odinhg/core>.

also a simplex in K . A **filtered simplicial complex** (over P) is a collection of simplicial complexes $\{(K_p, V)\}_{p \in P}$ such that $\{K_p\}_{p \in P}$ is a filtration of sets over P . We let $(0, \infty)$ denote the set of positive real numbers with the standard total ordering, and $[0, \infty]$ is the extended non-negative real line.

Definition 2.1 (Multicover Bifiltration). *Let (M, d) be a metric space, and $A \subseteq M$ a finite subspace. The **multicover bifiltration** $\text{Cov}(A)$ on A is the filtration over $(0, \infty) \times (0, \infty)^{\text{op}}$ whose sets for (real) parameters $r, k > 0$ are given as*

$$\text{Cov}_{r,k}(A) = \{x \in M \mid d(a, x) \leq r \text{ for at least } k \text{ points } a \in A\}. \quad (1)$$

We use closed balls instead of open balls like they do in [2, Def. 2.7]. However, as pointed out in [2, Remark 2.9], this does not matter for stability results since the two versions are 0-interleaved. Note that replacing k by its ceiling $\lceil k \rceil$ in (1) so that it reads “for at least $\lceil k \rceil$ points”, gives an equivalent definition. When we later discuss interleavings, it is convenient not to restrict k to integer values.

Definition 2.2 (Dissimilarity). *A **dissimilarity** (over $[0, \infty]$) is a function $F : S \times T \rightarrow [0, \infty]$ where S and T are sets.*

An example of a dissimilarity is the (extended) metric d of a metric space (M, d) .

Definition 2.3 (Balls). *For a dissimilarity $F : S \times T \rightarrow [0, \infty]$, the (**closed**) F -ball around $s \in S$ with radius $r \geq 0$ is the set*

$$B_F(s, r) = \{t \in T \mid F(s, t) \leq r\}.$$

We can construct a filtered simplicial complex from a dissimilarity as follows:

Definition 2.4 (Dowker Nerve). *The **Dowker nerve** $DF = \{(DF_r, S)\}_{r \in (0, \infty)}$ of a dissimilarity $F : S \times T \rightarrow [0, \infty]$ is the filtered simplicial complex where*

$$DF_r = \{\sigma \subseteq S \text{ finite} \mid \text{there exists } t \in T \text{ such that } F(s, t) \leq r \text{ for all } s \in \sigma\}.$$

For a topological space X , a **cover** is a collection of subsets $\mathcal{U} = \{U_i\}_{i \in I}$ of X such that $\bigcup_i U_i = X$. The cover \mathcal{U} is said to be **good** if the intersection $\bigcap_{j \in J} U_j$ is either empty or contractible for every finite subset $J \subseteq I$. The cover is **closed** if it consists of closed sets. If $X \subseteq \mathbb{R}^n$ is a Euclidean subspace, we say that the cover \mathcal{U} is **convex** if it consists of convex sets. Note that every convex cover is good.

Definition 2.5 (Nerve of a Cover). *Let $\mathcal{U} = \{U_i\}_{i \in I}$ be a cover of a space X . The **nerve** of \mathcal{U} is the simplicial complex $(N\mathcal{U}, I)$ where $N\mathcal{U}$ consists of the finite subsets J of I with the property that the intersection $\bigcap_{j \in J} U_j$ is nonempty.*

Lemma 2.6 (Functorial Nerve Lemma[1, Thm. 5.9 and Thm. 3.9]). *Let $\mathcal{U} = \{U_i\}_{i \in I}$ be a finite closed and convex cover of a Euclidean subspace $X \subseteq \mathbb{R}^n$. There exists a homotopy equivalence $\rho_X : X \rightarrow |N\mathcal{U}|$ from X to the geometric realization $|N\mathcal{U}|$ of the nerve $N\mathcal{U}$. Furthermore, if $Y \subseteq X$ is a subspace with a finite closed and convex cover $\mathcal{V} = \{V_i\}_{i \in I}$ such that $V_i \subseteq U_i$ for all $i \in I$, then the following diagram commutes up to homotopy:*

$$\begin{array}{ccc} Y & \xrightarrow{\rho_Y} & |N\mathcal{V}| \\ \downarrow & & \downarrow \\ X & \xrightarrow{\rho_X} & |N\mathcal{U}|. \end{array} \quad (2)$$

We observe that taking homology of the diagram (2) gives a diagram that commutes strictly, where the two horizontal maps are isomorphisms.

3 Core Bifiltration

In this section, we introduce the core bifiltration, using a specific family of dissimilarities. We also examine the Dowker nerves of these dissimilarities. The core bifiltration is a filtered space that is interleaved with the multicover bifiltration.

Definition 3.1 (Core Distance [5, Def. 5]). *Let $A \subseteq (M, d)$ be a finite metric subspace, let $k > 0$ and let $x \in M$. The k -core distance $\text{Core}_k^A(x)$ of x to A is the distance from x to one of its $\lceil k \rceil$ -th nearest neighbors in A . We use the convention that, if $k > |A|$, then the k -core distance is infinite.*

In particular, we note that if $x \in A$ and $0 < k \leq 1$, then the k -core distance $\text{Core}_k^A(x)$ is zero. Furthermore, it can be helpful to keep in mind the following three equivalent conditions related to the core distance as we will use them in later proofs: Let $A \subseteq (M, d)$ be a finite metric subspace, then for all $x \in M$ and $r, k > 0$, we have

$$\text{Core}_k^A(x) \leq r \iff \exists a_1, \dots, a_{\lceil k \rceil} \in A \text{ such that } d(a_i, x) \leq r \text{ for all } a_i \iff |B_d(x, r) \cap A| \geq k.$$

For HDBSCAN, the **mutual reachability distance** $G_k : A \times A \rightarrow [0, \infty]$, where

$$G_k(a, a') = \max \{ \text{Core}_k^A(a), \text{Core}_k^A(a'), d(a, a') \}, \quad (3)$$

is used in one of the main steps in the clustering algorithm [5, Def. 7 and Alg. 1]. We look at directed versions of this distance.

Definition 3.2 (Core Dissimilarity). *Let $A \subseteq (M, d)$ be a finite metric subspace, and let $k > 0$. The k -core dissimilarity of A in M is the dissimilarity $\Lambda_k : A \times M \rightarrow [0, \infty]$ given by*

$$\Lambda_k(a, x) = \max \{ \text{Core}_k^A(a), d(a, x) \}.$$

Following our convention, we denote balls of radius r centered at a with respect to the core dissimilarity by

$$B_{\Lambda_k}(a, r) = \{x \in M \mid \Lambda_k(a, x) \leq r\}. \quad (4)$$

Taking the union of such balls over A , we get a bifiltration.

Definition 3.3. *Let (M, d) be a metric space, and $A \subseteq M$ a finite subset. The **core bifiltration** $\text{Cr}(A)$ on A is a filtration over $(0, \infty) \times (0, \infty)^{op}$ whose sets $\text{Cr}_{r,k}(A)$ for (real) parameters $r, k > 0$ are given as the union of all Λ_k -balls of radius r , i.e.,*

$$\text{Cr}_{r,k}(A) = \bigcup_{a \in A} B_{\Lambda_k}(a, r).$$

The ball $B_{\Lambda_k}(a, r)$ is empty if $r < \text{Core}_k^A(a)$, and it is the metric ball $B_d(a, r)$ if $r \geq \text{Core}_k^A(a)$ (see Figure 2). In the case where $M = \mathbb{R}^n$ with the Euclidean metric $d = d_E$, this means that the intersections of such balls are either empty or contractible. In particular, the collection of balls $\mathcal{B}_{r,k} = \{B_{\Lambda_k}(a, r)\}_{a \in A}$ forms a closed and convex cover of $\text{Cr}_{r,k}(A)$.

Definition 3.4. *Let $A \subseteq (M, d)$ finite metric subspace. The **core Čech bifiltration** $\text{cC}(A) = \{(\text{cCr}_{r,k}(A), A)\}_{r,k > 0}$ on A is the filtered simplicial complex, filtered over $(0, \infty) \times (0, \infty)^{op}$, where $\text{cCr}_{r,k}(A) = D(\Lambda_k)_r = N\mathcal{B}_{r,k}$.*

Let us record the above discussion in a lemma, using the Nerve Lemma (Lemma 2.6).

Lemma 3.5. *Let $A \subseteq \mathbb{R}^n$ be a finite Euclidean subspace. For each $r, k > 0$, the space $\text{Cr}_{r,k}(A) \subseteq \mathbb{R}^n$ is homotopy equivalent to the geometric realization $|\text{cCr}_{r,k}(A)|$ of the simplicial complex $\text{cCr}_{r,k}(A)$.*

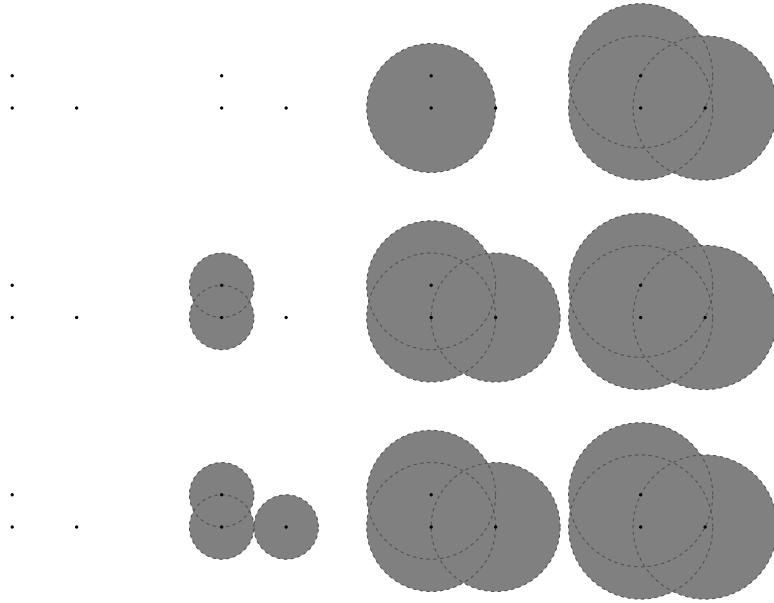


Figure 2: The core bifiltration with the union of Λ_k -balls shown in gray for different radii (increasing from left to right) and values of k where $A = \{(0, 0), (0, 1), (2, 0)\} \subseteq \mathbb{R}^2$. The top, middle and bottom rows correspond to $k = 3$, $k = 2$ and $k = 1$, respectively. The point cloud A and the boundaries of the metric balls are shown for clarity.

Note that the functorial part of the Nerve Lemma 2.6 gives that these degreewise homotopy equivalences induce isomorphisms between the persistent homology groups of $\text{Cr}(A)$ and $\text{cC}(A)$.

To connect the core bifiltration with the multicover bifiltration, we consider a second directed version of the mutual reachability distance (3), namely the dissimilarity $\Gamma_k : A \times M \rightarrow [0, \infty]$ where

$$\Gamma_k(a, x) = \max \{ \text{Core}_k^A(x), d(a, x) \}. \quad (5)$$

This dissimilarity is slightly less well-behaved, compared to Λ_k , as the balls $B_{\Gamma_k}(a, r)$ no longer have to be contractible even in the Euclidean case (see Figure 3). However, it is of interest for the following reason:

Lemma 3.6. *Let $A \subseteq (M, d)$ be a finite subset and let $r, k > 0$. The union of balls $\bigcup_{a \in A} B_{\Gamma_k}(a, r)$ is exactly the set $\text{Cov}_{r,k}(A)$ from the multicover bifiltration.*

Proof. Observe that asking for $x \in M$ to satisfy $\text{Core}_k^A(x) \leq r$ is equivalent to the existence of at least $\lceil k \rceil$ points a_i in A satisfying $d(a_i, x) \leq r$. Now, if $x \in B_{\Gamma_k}(a, r)$ for some $a \in A$, we have that $\text{Core}_k^A(x) \leq r$ so it follows from our observation that $x \in \text{Cov}_{r,k}(A)$. Conversely, if $x \in \text{Cov}_{r,k}(A)$ then again by the above observation we have that $\text{Core}_k^A(x) \leq r$, and $d(a, x) \leq r$ for at least one $a \in A$ since $\lceil k \rceil \geq 1$. \square

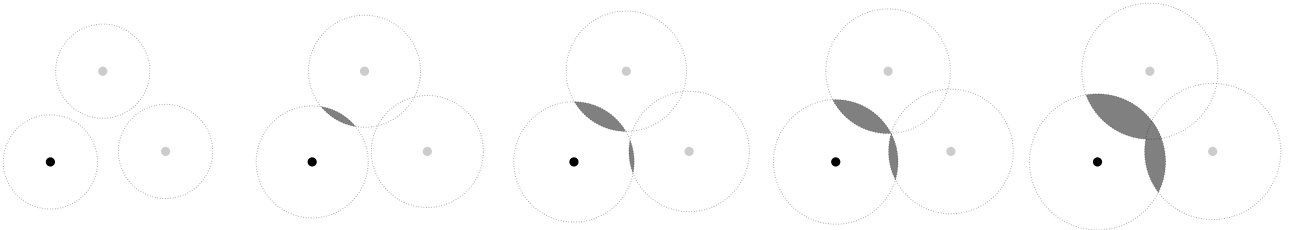


Figure 3: The Γ_2 -ball $B_{\Gamma_2}((0, 0), r)$ shown in gray as r increases from left to right, with $A = \{(0, 0), (1, \sqrt{3}), (2.1, 0.1)\}$.

So far, we have introduced the core dissimilarities Λ_k from which we defined the core bifiltration $\text{Cr}(A)$ (by taking unions of closed balls), and the core Čech bifiltration $\text{cC}(A)$ (by taking the Dowker

nerve). They are degreewise homotopy equivalent in the Euclidean case (Lemma 3.5). We end the section by presenting an interleaving between the multicover bifiltration $\text{Cov}(A)$ and the core bifiltration $\text{Cr}(A)$.

Theorem 3.7. *Let (M, d) be a metric space with a finite subspace $A \subseteq M$. The core bifiltration $\text{Cr}(A)$ and the multicover bifiltration $\text{Cov}(A)$ are interleaved as follows:*

$$i) \text{Cr}_{r,k}(A) \subseteq \text{Cov}_{2r,k}(A) \quad \text{and} \quad ii) \text{Cov}_{r,k}(A) \subseteq \text{Cr}_{2r,k}(A).$$

Proof. *i)* If x is a point in $\text{Cov}_{r,k}(A)$, then by Lemma 3.6 it is in some Γ_k -ball $B_{\Gamma_k}(a, r)$. In particular, $d(a, x) \leq r$ and $\text{Core}_k^A(x) \leq r$. This means that there are at least $\lceil k \rceil$ points $a_1, a_2, \dots, a_{\lceil k \rceil}$ in A whose distance to x is less than or equal to r . Now, $d(a_i, a) \leq d(a_i, x) + d(a, x) \leq 2r$, so the $\lceil k \rceil$ points $a_1, \dots, a_{\lceil k \rceil}$ have distance to a less than or equal to $2r$. Thus, $\text{Core}_k^A(a) \leq 2r$, and the point x is in $B_{\Lambda_k}(a, 2r) \subseteq \text{Cr}_{2r,k}(A)$.

ii) If x is a point in $\text{Cr}_{r,k}(A)$, then there exists a in A with $\text{Core}_k^A(a) \leq r$ and $d(a, x) \leq r$. Again, we can pick $\lceil k \rceil$ points $a_1, \dots, a_{\lceil k \rceil}$ in A whose distance to a is less than or equal to r . For these points we have $d(a_i, x) \leq d(a_i, a) + d(a, x) \leq 2r$, so the k -core distance $\text{Core}_k^A(x)$ is less than or equal to $2r$ and x is in the ball $B_{\Gamma_k}(a, 2r)$ which by Lemma 3.6 is a subset of $\text{Cov}_{2r,k}(A)$. \square

4 Alpha-Core Bifiltration

We now use the standard approach of intersecting with Voronoi cells, to get a smaller variation of the core bifiltration.

Definition 4.1. *Let $A \subseteq \mathbb{R}^n$ be a finite Euclidean subspace. The **Voronoi cell** $\text{Vor}_A(a)$ of $a \in A$ is the set of all points that are at least as close to a as to any other point in A , namely,*

$$\text{Vor}_A(a) = \{x \in \mathbb{R}^n \mid d_E(a, x) \leq d_E(a', x) \text{ for all } a' \in A\}.$$

Each Voronoi cell is closed and convex, so the collection $\text{Vor}(A) = \{\text{Vor}_A(a)\}_{a \in A}$ forms a closed and convex cover of \mathbb{R}^n . The nerve of $\text{Vor}(A)$ is often called the **Delaunay complex** of A . We recall that the balls $B_{\Lambda_k}(a, r)$ (from (4)) covering the core bifiltration $\text{Cr}_{r,k}(A)$ are either empty or closed metric balls $B_d(a, r)$. Euclidean balls are convex, so the closed **Voronoi balls**

$$W_{r,k}(a) := B_{\Lambda_k}(a, r) \cap \text{Vor}_A(a)$$

are either empty or convex, and thus they form a closed and convex cover of their union.

Definition 4.2. *Let $A \subseteq \mathbb{R}^n$ be a finite Euclidean subspace. The **alpha-core bifiltration** $\alpha\text{Cr}(A)$ of A is the bifiltration given by the union of Voronoi balls:*

$$\alpha\text{Cr}_{r,k}(A) = \bigcup_{a \in A} W_{r,k}(a) = \bigcup_{a \in A} (B_{\Lambda_k}(a, r) \cap \text{Vor}_A(a)).$$

The nerve of the cover $\mathcal{W}_{r,k} = \{W_{r,k}(a)\}_{a \in A}$ is homotopy equivalent to $\alpha\text{Cr}_{r,k}(A)$ by the Nerve Lemma 2.6, and it is contained in the Delaunay complex $N(\text{Vor}(A))$ whose size is $\mathcal{O}(|A|^{\lceil n/2 \rceil})$ [10, 14]. Unlike the standard Alpha complex, which is homotopy equivalent to the Čech complex, the same is not the case for the alpha-core and the core bifiltrations. However, we now show that they are interleaved.

Lemma 4.3. *Let $A \subseteq \mathbb{R}^n$ be a finite Euclidean subspace. The core bifiltration $\text{Cr}(A)$ and the alpha-core bifiltration $\alpha\text{Cr}(A)$ are interleaved as follows:*

$$\alpha\text{Cr}_{r,k}(A) \subseteq \text{Cr}_{r,k}(A) \subseteq \alpha\text{Cr}_{3r,k}(A).$$

Proof. It follows directly from $W_{r,k}(a) \subseteq B_{\Lambda_k}(a, r)$ that $\alpha\text{Cr}_{r,k}(A) \subseteq \text{Cr}_{r,k}(A)$. If $x \in \text{Cr}_{r,k}(A)$, then there exists $a' \in A$ such that $\text{Core}_k^A(a') \leq r$ and $d(a', x) \leq r$. Let $a \in A$ be such that $x \in \text{Vor}_A(a)$. Choose $\lceil k \rceil$ points $a_1, \dots, a_{\lceil k \rceil}$ in A with $d(a', a_i) \leq r$ for $i = 1, \dots, \lceil k \rceil$. Since $d(a, x) \leq d(a', x) \leq r$, the triangle inequality implies that

$$d(a, a_i) \leq d(a, x) + d(x, a') + d(a', a_i) \leq r + r + r = 3r,$$

and $\text{Core}_k^A(a) \leq 3r$ (see Figure 4). In particular, the point x is in $B_{\Lambda_k}(a, 3r)$ and thus also in $W_{3r,k}(a)$. We get that $\text{Cr}_{r,k}(A) \subseteq \alpha\text{Cr}_{3r,k}(A)$. \square

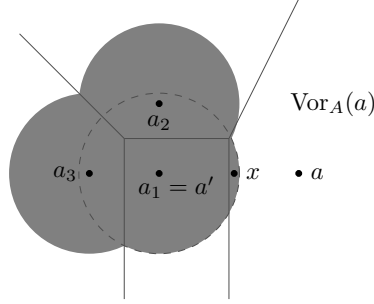


Figure 4: A diagram illustrating the proof of the second inclusion in Lemma 4.3 when $A \subseteq \mathbb{R}^2$ and $k = 3$. Observe that the distance $d(a, a_3)$ can get arbitrarily close to $3r$ meaning that the multiplicative interleaving factor of 3 is the best we can hope for.

Combining theorems 3.7 and 4.3 gives us an interleaving between the multicover and alpha-core bifiltrations. However, by considering the alpha-version of the Γ_k -balls (Γ_k defined in (5)) we can make this interleaving even stricter.

Lemma 4.4. *Let $A \subseteq \mathbb{R}^n$ be a finite Euclidean subspace. The multicover bifiltration $\text{Cov}(A)$ can be written as a union of Γ_k -Voronoi balls, i.e.,*

$$\text{Cov}_{r,k}(A) = \bigcup_{a \in A} (B_{\Gamma_k}(a, r) \cap \text{Vor}_A(a)).$$

Proof. The Γ_k -Voronoi balls are contained in the Γ_k -balls, so their union is contained in $\text{Cov}_{r,k}(A)$. Conversely, if $x \in \text{Cov}_{r,k}(A)$, then, by Lemma 3.6, $\text{Core}_k^A(x) \leq r$ and $d(a', x) \leq r$ for some $a' \in A$. Now, if $x \in \text{Vor}_A(a)$, then $d(a, x) \leq d(a', x) \leq r$ and so $x \in B_{\Gamma_k}(a, r) \cap \text{Vor}_A(a)$. \square

Theorem 4.5. *Let $A \subseteq \mathbb{R}^n$ be a finite Euclidean subspace. The alpha-core bifiltration $\alpha\text{Cr}(A)$ and the multicover bifiltration $\text{Cov}(A)$ are interleaved as follows:*

$$i) \alpha\text{Cr}_{r,k}(A) \subseteq \text{Cov}_{2r,k}(A), \quad ii) \text{Cov}_{r,k}(A) \subseteq \alpha\text{Cr}_{2r,k}(A).$$

Proof. *i)* Using Theorem 3.7, we get the inclusion $\alpha\text{Cr}_{r,k}(A) \subseteq \text{Cr}_{r,k}(A) \subseteq \text{Cov}_{2r,k}(A)$.

ii) Let $x \in \text{Cov}_{r,k}(A) = \bigcup_{a \in A} (B_{\Gamma_k}(a, r) \cap \text{Vor}_A(a))$. This means that $\text{Core}_k^A(x) \leq r$, so we can pick $a_1, \dots, a_{\lceil k \rceil}$ in A with $d(a_i, x) \leq r$ for all $i = 1, \dots, \lceil k \rceil$, and that there exists an $a \in A$ such that $x \in \text{Vor}_A(a)$ and $d(a, x) \leq r$. In particular, we have $d(a, a_i) \leq d(a, x) + d(x, a_i) \leq 2r$, and so $\text{Core}_k^A(a) \leq 2r$. Since $d(a, x) \leq r \leq 2r$ we get $x \in B_{\Lambda_k}(a, 2r)$, and since $x \in \text{Vor}_A(a)$ we get that x is in $\alpha\text{Cr}_{2r,k}(A)$. \square

In this section, we have derived interleaving results for the alpha-core bifiltration, enabling us to further derive alpha-core stability as a corollary of multicover stability in the subsequent section.

5 Stability for Core Bifiltration

Blumberg and Lesnick [2] give a stability result for the multicover bifiltration with respect to the *Prohorov distance*. In this section, we establish similar results for the core and alpha-core bifiltrations. For a finite metric subset $S \subseteq (M, d)$ and $\delta \geq 0$, we let S^δ denote the δ -**thickening** of S , namely the set

$$S^\delta = \{x \in M \mid \exists s \in S \text{ such that } d(s, x) \leq \delta\} = \bigcup_{s \in S} B_d(s, \delta).$$

Now, for finite metric subspaces $A, B \subseteq M$, the **(counting) Prohorov distance** between them is

$$d_P(A, B) = \sup_{S \subseteq M \text{ closed}} \inf \left\{ \delta \geq 0 \mid |S \cap A| \leq |S^\delta \cap B| + \delta \text{ and } |S \cap B| \leq |S^\delta \cap A| + \delta \right\}.$$

By the triangle inequality, the δ -thickening of a metric ball of radius r is included in the metric ball of radius $r + \delta$, i.e., $B_d(x, r)^\delta \subseteq B_d(x, r + \delta)$ for all $x \in M$.

Theorem 5.1 (Multicover Stability [2, Rmk 3.2 for Thm 1.6]). *Let $A, B \subseteq (M, d)$ be finite metric subspaces and let $\delta > d_P(A, B)$. For all $r > 0$ and all $k > \delta$ we have inclusions*

$$\text{Cov}_{r,k}(A) \subseteq \text{Cov}_{r+\delta, k-\delta}(B) \quad \text{and} \quad \text{Cov}_{r,k}(B) \subseteq \text{Cov}_{r+\delta, k-\delta}(A).$$

Proof. We show the first inclusion, the second is symmetric. Let $x \in \text{Cov}_{r,k}(A)$. This is true if and only if $k \leq |B_d(x, r) \cap A|$. Using our assumption and the fact that $B_d(x, r)^\delta \subseteq B_d(x, r + \delta)$ we have

$$k \leq |B_d(x, r) \cap A| \leq |B_d(x, r)^\delta \cap B| + \delta \leq |B_d(x, r + \delta) \cap B| + \delta.$$

In particular, we get that $k - \delta \leq |B_d(x, r + \delta) \cap B|$, so $x \in \text{Cov}_{r+\delta, k-\delta}(B)$. \square

Using a similar approach, we get stability for the core bifiltration:

Theorem 5.2 (Core Stability). *Let $A, B \subseteq (M, d)$ be finite metric subspaces and let $\delta > d_P(A, B)$. For all $r > 0$ and all $k > \delta$ we have inclusions*

$$\text{Cr}_{r,k}(A) \subseteq \text{Cr}_{2r+2\delta, k-\delta}(B) \quad \text{and} \quad \text{Cr}_{r,k}(B) \subseteq \text{Cr}_{2r+2\delta, k-\delta}(A).$$

Proof. Let $x \in \text{Cr}_{r,k}(A)$. This is true if and only if there exists an $a \in A$ such that $d(a, x) \geq r$ and $k \leq |B_d(a, r) \cap A|$. If $a \in A$ is such a point, then

$$k \leq |B_d(a, r) \cap A| \leq |B_d(a, r)^\delta \cap B| + \delta \leq |B_d(a, r + \delta) \cap B| + \delta. \quad (6)$$

In particular, we have $0 < k - \delta \leq |B_d(a, r + \delta) \cap B|$, so let b be an element in the intersection $B_d(a, r + \delta) \cap B$. By the triangle inequality, we have $B_d(a, r + \delta) \subseteq B_d(b, 2r + 2\delta)$ and $d(b, x) \leq d(b, a) + d(a, x) \leq 2(r + \delta)$. So, $k - \delta \leq |B_d(b, 2r + 2\delta) \cap B|$ and $d(b, x) \leq 2r + 2\delta$. Thus $x \in \text{Cr}_{2r+2\delta, k-\delta}(B)$. \square

Combining Theorem 5.1 with Theorem 4.5, we get the following stability result for the alpha-core bifiltration.

Corollary 5.3 (Alpha-Core Stability). *Let $A, B \subseteq \mathbb{R}^n$ be finite Euclidean subspaces and let $\delta > d_P(A, B)$. For all $r > 0$ and $k > \delta$, we have inclusions*

$$\alpha \text{Cr}_{r,k}(A) \subseteq \alpha \text{Cr}_{4r+2\delta, k-\delta}(B) \quad \text{and} \quad \alpha \text{Cr}_{r,k}(B) \subseteq \alpha \text{Cr}_{4r+2\delta, k-\delta}(A).$$

\square

Blumberg and Lesnick [2, Def. 2.13] also consider a *normalized* version of the multicover bifiltration. We can define normalized versions of all our filtrations by letting

$$\begin{aligned} \text{Cov}_{r,s}^N(A) &= \text{Cov}_{r, s|A|}(A), \\ \text{Cr}_{r,s}^N(A) &= \text{Cr}_{r, s|A|}(A), \quad \text{and} \\ \alpha \text{Cr}_{r,s}^N(A) &= \alpha \text{Cr}_{r, s|A|}(A). \end{aligned}$$

In practice, we are often in a situation where $|A| \neq |B|$. Then, it makes more sense to consider the normalized versions listed above so that the second parameters in the corresponding bifiltrations are comparable. The **normalized Prohorov distance** between finite metric subspaces $A, B \subseteq M$ is defined as

$$d_P^N(A, B) = \sup_{S \subseteq M \text{ closed}} \inf \left\{ \delta \geq 0 \mid \frac{|S \cap A|}{|A|} \leq \frac{|S^\delta \cap B|}{|B|} + \delta \text{ and } \frac{|S \cap B|}{|B|} \leq \frac{|S^\delta \cap A|}{|A|} + \delta \right\}.$$

As with the unnormalized case, the stability for normalized multicover bifiltration in [2, Thm. 1.6] also extends to a stability for the normalized core- and alpha-core bifiltrations.

Theorem 5.4 (Normalized Stability). *Let $A, B \subseteq \mathbb{R}^n$ be finite Euclidean subspaces and let $\delta > d_P^N(A, B)$. For all $r > 0$ and $s > \delta$, we have inclusions*

$$\begin{aligned} \text{Cov}_{r,s}^N(A) &\subseteq \text{Cov}_{r+\delta, s-\delta}^N(B), & \text{Cov}_{r,s}^N(B) &\subseteq \text{Cov}_{r+\delta, s-\delta}^N(A); \\ \text{Cr}_{r,s}^N(A) &\subseteq \text{Cr}_{2r+2\delta, s-\delta}^N(B), & \text{Cr}_{r,s}^N(B) &\subseteq \text{Cr}_{2r+2\delta, s-\delta}^N(A); \\ \alpha\text{Cr}_{r,s}^N(A) &\subseteq \alpha\text{Cr}_{4r+2\delta, s-\delta}^N(B), & \alpha\text{Cr}_{r,s}^N(B) &\subseteq \alpha\text{Cr}_{4r+2\delta, s-\delta}^N(A). \end{aligned}$$

6 Experiments

We have implemented code to compute the persistent homology of the core and alpha-core bifiltrations along a line in parameter space. The implementation, available at <https://github.com/odinhg/core>, includes code demonstrating its use, and code to reproduce the experiments reported in this section. The implementation uses the GUDHI library [16, 12, 13], which allows for easy computation of the corresponding persistent homology modules and the bottleneck distances between them.

We compute the persistent homology of the core and alpha-core bifiltration along the line $k = g(r) = -\frac{k_{\max}}{r_{\max}}r + k_{\max}$ where k_{\max} and r_{\max} are positive real numbers. Note that for non-integer values of k , we round up to the nearest integer, i.e., we compute persistence along the piece-wise constant function $k = \lceil g(r) \rceil$. Of course, we can also compute the core and alpha-core bifiltrations for k fixed ($r_{\max} = +\infty$).

In our experiments, we choose r_{\max} to be the diameter of the input point cloud and set the parameter $k_{\max} = \max\{1, \lfloor s_{\max}|X| \rfloor\}$ with $s_{\max} \in \{0, 0.001, 0.01, 0.1\}$ so that k_{\max} scales with the number of points in the input point cloud. Similarly, in the fixed- k case, we let $k = \max\{1, \lceil s|X| \rceil\}$.

We consider five point cloud datasets in our experiments: **Torus 1**, **Torus 2**, **Sphere**, **Circle** and **Circles**. See Figure 5 for a visualization of four of these datasets. We construct our point cloud datasets as follows: For an underlying manifold $M \subseteq \mathbb{R}^d$ (see Table 1 for an overview of the manifolds used for the different datasets), we first uniformly sample a point cloud of size n from the manifold M . We then perturb the points according to a normal distribution having mean $\mu = 0$ and standard deviation $\sigma = 0.07$ to obtain a perturbed sample Z . In the last step, we uniformly sample m points Y from the smallest axis parallel hyperbox containing Z , and obtain our point cloud dataset $X = X(M, m, n, \sigma) = Z \cup Y$. We think of Z as a noisy signal and Y as background noise. Figure 6 shows persistence diagrams for the alpha-core bifiltration for various values of k_{\max} for the **Torus 2** dataset.

Dataset name	Manifold M
Torus 1	The 2-torus embedded in \mathbb{R}^3 .
Torus 2	The Clifford torus $S^1 \times S^1$ in \mathbb{R}^4 .
Sphere	The 2-sphere $S^2 \subseteq \mathbb{R}^3$.
Circle	The 1-sphere $S^1 \subseteq \mathbb{R}^2$.
Circles	The union of two circles with radii 0.5 and 1 in \mathbb{R}^2 .

Table 1: The underlying manifolds used to generate the five datasets.

As a ground truth for a sample $X = X(M, m, n, \sigma)$, we use the Čech persistent homology of a uniform sample $X_t = X(M, 0, m + n, 0)$ from M of size $n + m$ without any perturbation or added

noise. In practice, we compute the Čech persistence using alpha-core with $k = 1$. To compare the alpha-core persistence of the noisy sample against the ground truth Čech persistence, we compute the bottleneck distance between their corresponding persistence diagrams. The computed bottleneck distances for $k = g(r)$ and k fixed are listed in Table 2 and Table 3 in Appendix A, respectively. In addition, we report runtimes for computing alpha-core persistence on the **Torus 1** dataset in Table 4 for different choices of k and point cloud sizes.

Based on our experiments, we see that choosing $s > 0$, corresponding to $k > 1$, in most cases gives persistence diagrams closer to the ground truth in terms of the bottleneck distance than for $k = 1$. Moreover, in most cases, the persistence along a sloped line yields slightly smaller bottleneck distance than persistence along lines with constant s . However, the difference between the bottleneck distances in these two cases is small in all of our experiments. We also note that the optimal choice of s depends both on the homological dimension and on the shape of the point clouds.

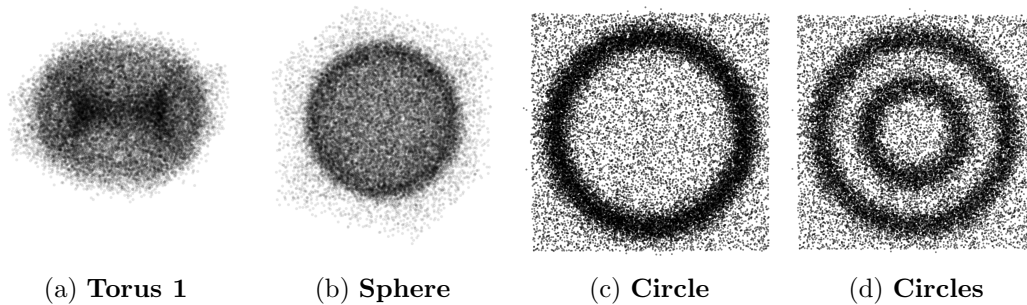


Figure 5: Four of the point cloud datasets used in our experiments with $\sigma = 0.07$ (perturbation strength), $n = 20000$ (signal) and $m = 10000$ (noise).

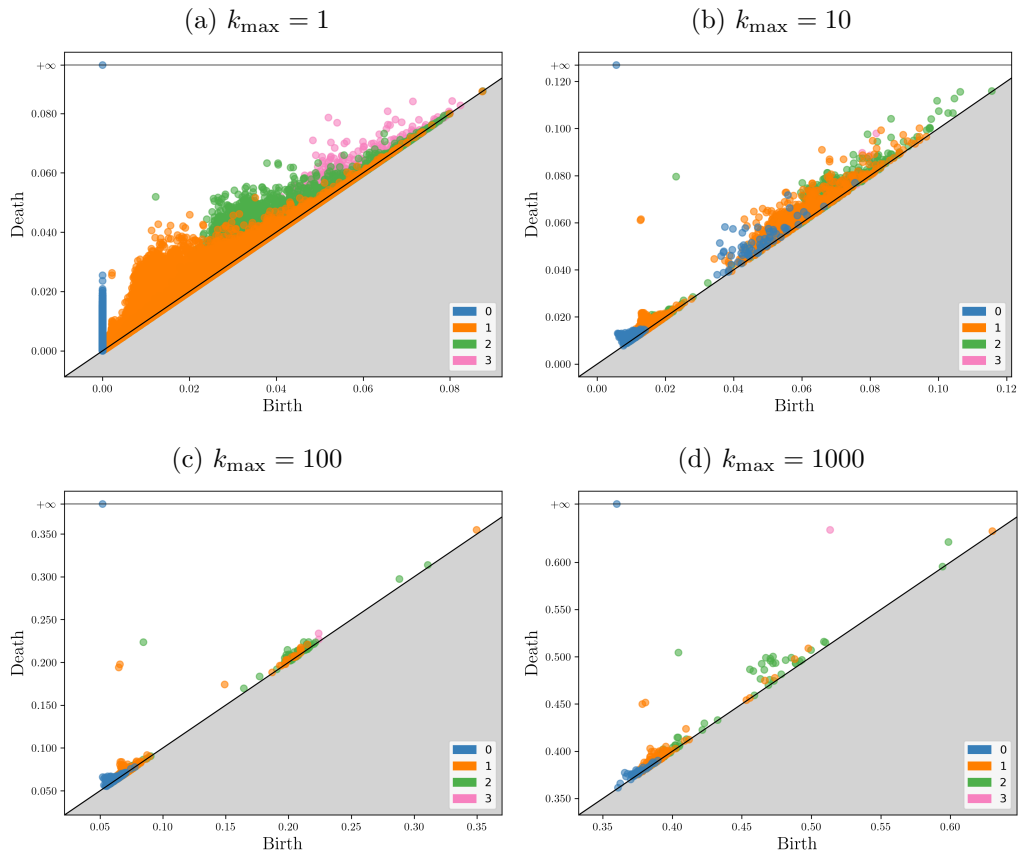


Figure 6: Persistence diagrams for the alpha-core bifiltration of the **Torus 2** (Clifford torus) dataset with $r_{\max} = \text{diam}(X) \approx 4.10$. In this example, we have a 1 : 1 signal-to-noise ratio with $n = m = 10000$, and observe that increasing k_{\max} strengthens the separation between noise and those persistence pairs we expect to see for a torus. The different colours correspond to the different homological dimensions.

7 Conclusions

We have introduced the core and alpha-core bifiltrations and shown how they relate to the multicover bifiltration via interleavings. In addition, we have shown how the stability results for the multicover bifiltration directly extends to stability for the core and alpha-core bifiltrations. For the core bifiltration, we have established a stability result stronger than the transferred multicover stability by giving a direct proof. We have also presented experimental results showing how alpha-core persistence can be useful for analyzing relatively large point clouds in cases where robustness to noise is desired.

In future work, it would be interesting to see if these stability results can be strengthened further. It would also be interesting to consider stability with respect to metrics besides the Prohorov distance, and conditions on the point cloud giving stability for a fixed density parameter k .

In the applied direction, we believe it would be worthwhile to look into how we can best choose the line to compute persistence along, and also explore how alpha-core persistence can be applied to real-world datasets.

A Supporting Tables for Experimental Results

n, m	10000, 10000				10000, 1000				10000, 100			
	s_{\max}	0	0.001	0.01	0.1	0	0.001	0.01	0.1	0	0.001	0.01
Torus 1												
Dim 0	0.109	0.161	0.614	1.475	0.187	0.114	0.518	1.381	0.273	0.118	0.509	1.420
Dim 1	0.977	0.977	0.977	0.977	0.968	0.968	0.554	0.968	0.967	0.662	0.546	0.967
Dim 2	0.425	0.425	0.425	0.425	0.270	0.183	0.388	0.388	0.136	0.125	0.390	0.391
Torus 2												
Dim 0	0.086	0.131	0.404	0.958	0.147	0.089	0.324	0.973	0.178	0.092	0.308	0.986
Dim 1	0.487	0.487	0.414	0.487	0.482	0.482	0.338	0.482	0.478	0.405	0.387	0.482
Dim 2	0.445	0.445	0.372	0.445	0.441	0.411	0.303	0.441	0.330	0.227	0.291	0.439
Dim 3	0.207	0.207	0.207	0.207	0.207	0.207	0.207	0.154	0.207	0.207	0.207	0.207
Sphere												
Dim 0	0.042	0.073	0.227	0.635	0.091	0.055	0.190	0.589	0.146	0.049	0.177	0.590
Dim 1	0.029	0.016	0.016	0.016	0.044	0.020	0.020	0.020	0.020	0.022	0.022	0.022
Dim 2	0.475	0.475	0.475	0.475	0.470	0.470	0.302	0.470	0.465	0.423	0.278	0.465
Circle												
Dim 0	0.012	0.014	0.074	0.371	0.034	0.020	0.053	0.312	0.106	0.010	0.052	0.301
Dim 1	0.499	0.499	0.499	0.393	0.499	0.499	0.499	0.357	0.499	0.499	0.263	0.338
Circles												
Dim 0	0.125	0.125	0.092	0.377	0.125	0.114	0.088	0.356	0.064	0.125	0.098	0.356
Dim 1	0.249	0.249	0.249	0.249	0.248	0.248	0.159	0.248	0.248	0.248	0.219	0.248

Table 2: Bottleneck distances between the ground truth persistence diagrams and the alpha-core persistence diagrams along the line $g(r)$ determined by s_{\max} , $n + m$ and the diameter of the input point cloud.

n, m	10000, 10000				10000, 1000				10000, 100			
	s	0	0.001	0.01	0.1	0	0.001	0.01	0.1	0	0.001	0.01
Torus 1												
Dim 0	0.109	0.161	0.603	1.392	0.187	0.114	0.505	1.302	0.273	0.118	0.501	1.355
Dim 1	0.977	0.977	0.977	0.977	0.968	0.968	0.545	0.968	0.967	0.684	0.549	0.967
Dim 2	0.425	0.425	0.425	0.425	0.270	0.183	0.387	0.388	0.136	0.125	0.391	0.391
Torus 2												
Dim 0	0.086	0.131	0.388	0.901	0.147	0.089	0.315	0.895	0.178	0.092	0.300	0.879
Dim 1	0.487	0.487	0.421	0.487	0.482	0.482	0.343	0.482	0.478	0.409	0.387	0.482
Dim 2	0.445	0.445	0.390	0.445	0.441	0.420	0.288	0.441	0.330	0.227	0.277	0.439
Dim 3	0.207	0.207	0.207	0.207	0.207	0.207	0.207	0.178	0.207	0.207	0.207	0.207
Sphere												
Dim 0	0.042	0.073	0.220	0.595	0.091	0.055	0.186	0.548	0.146	0.049	0.175	0.544
Dim 1	0.029	0.016	0.016	0.016	0.044	0.020	0.020	0.020	0.020	0.022	0.022	0.022
Dim 2	0.475	0.475	0.475	0.475	0.470	0.470	0.340	0.470	0.465	0.423	0.283	0.465
Circle												
Dim 0	0.012	0.014	0.073	0.342	0.034	0.020	0.053	0.288	0.106	0.010	0.051	0.275
Dim 1	0.499	0.499	0.499	0.432	0.499	0.499	0.499	0.328	0.499	0.499	0.270	0.308
Circles												
Dim 0	0.125	0.125	0.096	0.357	0.125	0.114	0.092	0.340	0.064	0.125	0.099	0.341
Dim 1	0.249	0.249	0.249	0.249	0.248	0.248	0.162	0.248	0.248	0.248	0.223	0.248

Table 3: Bottleneck distances between the ground truth persistence diagrams and the alpha-core persistence diagrams for a fixed s (and k).

$n + m$	Fixed k			
	10	100	1000	10000
10000	1.11	1.14	1.72	7.86
20000	2.32	2.42	3.59	16.90
30000	3.57	3.75	5.58	26.71
40000	4.85	5.08	7.50	35.15
50000	6.17	6.53	9.76	47.29
60000	7.51	7.91	11.70	56.64

Table 4: Runtimes (in seconds) for computing alpha-core persistence on the **Torus 1** dataset with $n = m = |X|/2$ and $\sigma = 0.07$. The computations were conducted on an Intel Core i5-6300U (at 2.40 GHz) CPU with 16 GB RAM. The minimum runtime out of 10 runs is reported in the table.

References

- [1] Ulrich Bauer, Michael Kerber, Fabian Roll, and Alexander Rolle. A unified view on the functorial nerve theorem and its variations. *Expositiones Mathematicae*, 41(4):125503, December 2023. URL: <http://dx.doi.org/10.1016/j.exmath.2023.04.005>, doi:10.1016/j.exmath.2023.04.005.
- [2] Andrew J Blumberg and Michael Lesnick. Stability of 2-parameter persistent homology. *Foundations of Computational Mathematics*, pages 1–43, 2022.
- [3] Magnus Bakke Botnan and Michael Lesnick. An introduction to multiparameter persistence, 2023. [arXiv:2203.14289](https://arxiv.org/abs/2203.14289).
- [4] Mickaël Buchet, Bianca B. Dornelas, and Michael Kerber. Sparse Higher Order Čech Filtrations. In *39th International Symposium on Computational Geometry (SoCG 2023)*, volume 258 of *Leibniz International Proceedings in Informatics (LIPIcs)*, pages 20:1–20:17, Dagstuhl, Germany, 2023. Schloss Dagstuhl – Leibniz-Zentrum für Informatik. doi:10.4230/LIPIcs.SoCG.2023.20.
- [5] Ricardo J.G.B. Campello, Davoud Moulavi, and Joerg Sander. Density-based clustering based on hierarchical density estimates. In *Advances in Knowledge Discovery and Data Mining*, pages 160–172, Berlin, Heidelberg, 2013. Springer Berlin Heidelberg.
- [6] Gunnar Carlsson and Afra Zomorodian. The theory of multidimensional persistence. In *Computational geometry (SCG’07)*, pages 184–193. ACM, New York, 2007. doi:10.1145/1247069.1247105.
- [7] René Corbet, Michael Kerber, Michael Lesnick, and Georg Osang. Computing the multicover bifiltration. *Discrete & Computational Geometry*, 70(2):376–405, Sep 2023. doi:10.1007/s00454-022-00476-8.
- [8] Herbert Edelsbrunner and Georg Osang. The multi-cover persistence of euclidean balls. *Discrete & Computational Geometry*, 65(4):1296–1313, Jun 2021. doi:10.1007/s00454-021-00281-9.
- [9] Herbert Edelsbrunner and Georg Osang. A simple algorithm for higher-order delaunay mosaics and alpha shapes. *Algorithmica*, 85(1):277–295, Jan 2023. doi:10.1007/s00453-022-01027-6.
- [10] Victor Klee. On the number of vertices of a convex polytope. *Canadian Journal of Mathematics*, 16:701–720, 1964. doi:10.4153/CJM-1964-067-6.
- [11] Michael Lesnick and Matthew Wright. Interactive visualization of 2-d persistence modules, 2015. [arXiv:1512.00180](https://arxiv.org/abs/1512.00180).
- [12] Clément Maria. Filtered complexes. In *GUDHI User and Reference Manual*. GUDHI Editorial Board, 2015. URL: http://gudhi.gforge.inria.fr/doc/latest/group__simplex__tree.html.

- [13] Vincent Rouvreau. Alpha complex. In *GUDHI User and Reference Manual*. GUDHI Editorial Board, 2015. URL: http://gudhi.gforge.inria.fr/doc/latest/group__alpha__complex.html.
- [14] Raimund Seidel. The upper bound theorem for polytopes: an easy proof of its asymptotic version. *Computational Geometry*, 5(2):115 – 116, 1995. URL: <http://www.sciencedirect.com/science/article/pii/092577219500013Y>, doi:10.1016/0925-7721(95)00013-Y.
- [15] Donald R. Sheehy. A multicover nerve for geometric inference. In *CCCG: Canadian Conference in Computational Geometry*, 2012.
- [16] The GUDHI Project. *GUDHI User and Reference Manual*. GUDHI Editorial Board, 2015. URL: <http://gudhi.gforge.inria.fr/doc/latest/>.